ELSEVIER

Impacts of increased urbanization on surface temperature, vegetation, and aerosols over Bengaluru, India

Heather S. Sussman [*], Ajay Raghavendra, Liming Zhou

Department of Atmospheric and Environmental Sciences, University at Albany, State University of New York, 1400 Washington Ave. Albany, NY 12222, USA

A B S T R A C T

Bengaluru is India's third largest city by population and has been noted as a prime example of rapid urbanization due to the increased presence of the information technology industry. Urban areas are typically characterized by (1) higher land surface temperatures (LST) when compared to their surroundings, known as the urban heat island (UHI) effect, and (2) lower vegetation spatial extent and density. However, an observational study exploring the impacts of increased urbanization on surface temperature and vegetation in Bengaluru during different seasons and time of day is lacking. Here, satellite products of LST, Enhanced Vegetation Index (EVI), aerosol optical depth, and land cover from the MODerate Resolution Imaging Spectroradiometer (MODIS) were used to assess changes in EVI and daytime and nighttime LST over Bengaluru and surrounding non-urban areas from 2003 to 2018 for the dry (December–February) and wet (August–October) seasons. Results showed that the amount of urbanized land increased by 15% from 2003 to 2018. The mean UHI intensity was found to be of greatest magnitude during the dry season at nighttime, and an UHI was also observed for the wet season during both daytime and nighttime hours. The UHI intensity exhibited an increasing trend in the dry season nighttime and wet season daytime and nighttime, suggesting an enhanced UHI effect with increased urban area. Results further show an absence of a daytime UHI during the dry season with a significant daytime cooling trend most likely attributable to an increase in aerosols, which act to limit daytime surface warming. Understanding the relationships among urbanization, UHI intensity, vegetation, and aerosols, and how they change with time could be useful to project future UHI impacts in Bengaluru.

1. Introduction

Cities are home to more than half of the world's population (Kim and Baik, 2005; Grimm et al., 2008). As many cities continue to expand, there are considerable land cover/land-use changes that occur due to urbanization. Additionally, the accessibility for people to see and enjoy nature decreases with increased urbanization as well as the potential for vegetation to thrive (Andersson, 2006). Consequently, there exists a need to understand how urbanization may impact the environment (e.g., temperature, local and regional climate, air and water quality, vegetation, and drainage) and associated human impacts (e.g., heat exhaustion and respiratory diseases), especially in developing areas where urbanization rates are rapid and generally understudied (Baud and De Wit, 2008).

It is well observed that urban areas have higher surface and air temperatures than surrounding suburban and non-urban areas, a phenomenon known as the urban heat island (UHI) effect. There are various factors that influence UHI intensity including land surface properties, local climate, season, time of day, the geographical location of the city, the size of the city in terms of both area and population, and anthropogenic heat (Kim and Baik, 2005). For example, Oke (1973) and Park (1986) illustrated that UHI intensity increases as a city's population increases. Ichinose et al. (1999) showed the seasonal relevance of anthropogenic heat and how UHI intensity is greater in winter than during the summer. Additionally, cities tend to have less vegetation, higher heat capacities, and more buildings, asphalt sidewalks, and roads compared to non-urban areas. These urban surface properties result in higher heat storage during the daytime and thus more heating at nighttime than natural surfaces (Kim and Baik, 2002). Also, urban surfaces are characterized by lower evapotranspiration rates and a higher Bowen ratio (i.e., the ratio between sensible heat fluxes and latent heat fluxes), which help urban surfaces to warm faster than suburban and non-urban surfaces during the daytime (Taha, 1997). However, this daytime warming effect could be weakened as planetary boundary layer

(PBL) mixing, which is strongest during the day, is enhanced due to increased urban surface roughness (Garratt, 1994). This helps to dissipate more surface heat upward (Xia et al., 2016) and result in less warming contrast between urban and non-urban surfaces (Miao et al., 2009). Previous estimates indicate that UHI intensity is strongly regionally dependent and varies greatly among cities due to their differences in the aforementioned controlling factors (e.g., Kim and Baik, 2005). In general, surface UHI intensity is greater at daytime on an annual scale as shown by Peng et al. (2012), where they analyzed 419 cities using satellite data and found global surface UHI intensity to be highest in the daytime for 64% of the cities. However, the 36% of the cities that had a higher UHI at nighttime were typically clustered in western and southern Asia and northern Africa, i.e., in developing regions of the world, where urbanization is typically understudied (Baud and De Wit, 2008). Therefore, attention should be given to urbanizing cities within these developing areas to determine why they exhibit a higher UHI intensity at nighttime rather than daytime.

Additionally, increased urbanization reduces vegetation density and spatial extent and lowers evapotranspiration, which further amplifies the UHI effect (Peng et al., 2012; Zhou et al., 2004, 2007). However, if cities work to maintain or augment the area of green spaces, the increased vegetation density and spatial extent generates increased evaporative cooling during the daytime (Peng et al., 2012), which decreases urban temperatures (Weng et al., 2004; Hung et al., 2005), and thus reduces the daytime UHI. Therefore, vegetation greenness needs to be quantified when analyzing the UHI effect of a city to determine whether it promotes a warming or cooling effect. Satellite measured vegetation indices such as the normalized difference vegetation index (NDVI) are commonly used to quantify the abundance and energy absorption by leaf pigments such as chlorophyll (Zhou et al., 2001) and is also indicative of an urban climate (Gallo et al., 1993; Gallo and Owen, 1999).

Another influence on UHI intensity is aerosols. Aerosols can either scatter or absorb visible and near-infrared (IR) radiation (i.e., the wavelengths where most of the solar radiation is contained). Urban areas typically have more pollutant aerosols than non-urban (Tie and Cao, 2009; Kanakidou et al., 2011), which are typically in the form of black carbon (BC). BC aerosols are generated from the incomplete combustion of vehicular and industrial fuels (Koelmans et al., 2006) and have strong solar radiation absorption properties (Jacobson, 2001; Ramachandran and Kedia, 2010), and thus can reduce land surface temperature (LST) during the daytime (Cusack et al., 1998; Lacis and Mishchenko, 1995; Qian et al., 2003, 2006). Jin et al. (2010) recently showed that a high aerosol optical depth (AOD) can reduce absorption of sunlight at the surface by $40-100 \, \text{Wm}^{-2}$ and reduce LST over urban areas by $1-2 \, \text{K}$ when compared to non-urban surroundings over Beijing. Therefore, increased AOD can reduce solar heating at daytime, and this cooling can cancel or exceed the UHI effect. Despite that rapid urbanization often causes increased pollution, and thus increased aerosols in urban areas, AOD and its relation to UHI intensity has rarely been investigated.

UHI intensity has been quantified as the difference in air temperature between two weather stations, one urban and one nearby non-urban (Gallo and Owen, 1999; Kalnay and Cai, 2003; Petersen, 2003; Zhou et al., 2004; Yang et al., 2013; Dienst et al., 2019). However, due to a low density of weather stations over many regions, satellite data have recently used LST to characterize spatiotemporal structures of UHI with sufficient resolution to distinguish between urban centers and non-urban surroundings and provide global coverage at high resolution (e.g., Hung et al., 2005; Peng et al., 2012; Anniballe et al., 2014; Fathi et al., 2019). LST has been shown to be similar to air temperature for both urban and non-urban areas (Prihodko and Goward, 1997; Mostovoy et al., 2006; Cheng et al., 2008). However, the UHI intensity measured using LST compared to the UHI intensity measured using air temperature has been shown to be larger in magnitude, although both data sources show UHI impacts (Anniballe et al., 2014; Schwarz et al.,

2012). Using either metric, UHI impacts have been extensively studied in various cities using satellite products such as Houston, Texas (Streutker, 2003), Shanghai, China (Cui and Shi, 2012), Milan, Italy (Anniballe et al., 2014), among others, in terms of their magnitude in relation to the factors listed in Kim and Baik (2005).

United Nations (2018) projects an increase from 18 to 43 megacities (i.e., a city with over 10 million inhabitants) by 2030, with most of them in developing countries such as India, China, and Nigeria. Together, these three countries are projected to account for 35% of the world's urban population growth between 2018 and 2050 (United Nations, 2018). Focusing on India, extreme urban growth in recent decades has transformed a mainly rural population and agricultural-based economy into a rapidly industrializing society accompanied by significant urbanization (Baud and De Wit, 2008). In particular, Bengaluru (12.97°N, 77.59°E), which is located in southern India on the Deccan Plateau at an elevation of 900 m above sea level, is India's third most populous city and has been noted as an excellent example of rapid urbanization (Sudhira et al., 2007; Sudhira and Nagendra, 2013). According to the most recent Census of India (2011), Bengaluru has a population of approximately 10 million, which represents a 47.18% increase from the total population in 2001 at the time of the previous census report. Additionally, Bengaluru was nicknamed the "*Garden City*" due to its lush greenery and presence of public parks. However, in recent years, the information technology industry has been encroaching on this greenness through the development of new infrastructure, and the creation of new jobs and housing projects. Now, Bengaluru is often referred to as India's "*Silicon City*" (Sudhira et al., 2007).

Despite rapid urbanization, the UHI intensity of Bengaluru has yet to be thoroughly quantified. To our knowledge, only Ramachandra and Kumar (2010) and Ambinakudige (2011) have quantified LST and NDVI changes over Bengaluru so far. Ramachandra and Kumar (2010) determined the mean annual LST in Bengaluru over different surface properties (e.g., varying degrees of urban, vegetated, and wet) using satellite data from Landsat in the 1990s and the MODerate Resolution Imaging Spectroradiometer (MODIS) in the early 2000s. Ambinakudige (2011) used MODIS LST data from March 2000 and 2003 to determine the minimum, maximum, mean, and standard deviation of LST on different surfaces in Bengaluru. Both studies found NDVI to decrease within the city. While both studies showed that an UHI does exist in Bengaluru and its intensity will likely increase with more urbanization, these studies did not account for seasonality and the diurnal cycle, which are critical to the understanding of UHIs in tropical Asian cities due to varying precipitation amounts throughout the year and large diurnal variations in temperature (Hung et al., 2005). Also, their usage of satellite remote sensing datasets were not the most up-to-date. Furthermore, NDVI could become saturated over dense vegetation and during the peak growing season (Zhou et al., 2014), and thus may not be the most reliable vegetation index. Additionally, previous works have shown that AOD has increased in India, especially during the dry season (e.g., Latha and Badarinath, 2003, 2005; Safai et al., 2007). In Bengaluru, an increase in atmospheric aerosols due to higher air pollution from automobiles has been observed (Ramachandran et al., 2012). Furthermore, Pandey et al. (2014) showed that increased AOD can induce an urban cool island during the dry months in New Delhi, India since aerosols cannot be quickly removed by wet deposition during this time. Since the effect of AOD on UHI intensity is a relatively new area of investigation (Pandey et al., 2014), there is interest to see if the UHI in Bengaluru acts in a similar manner to New Delhi when considering AOD since it was neglected in Ramachandra and Kumar (2010) and Ambinakudige (2011). Overall, Bengaluru's urbanization is unique in that urbanization impacts surface temperature, vegetation, and aerosols, thus making the city an excellent case study to see how these variables interact.

There exists opportunity to gain a better understanding of urbanization impacts over Bengaluru using the most up-to-date satellite remote sensed products, namely products from MODIS. While weather stations do exist in the Bengaluru area, coverage is sparse (Mendelsohn et al.,

2007), and therefore these in-situ measurements would not be suitable for a study of this nature. To overcome the data quality limitations of NDVI, another vegetation greenness index, namely the enhanced vegetation index (EVI), can be used as a proxy for vegetation health and abundance as well as be an indicator of urban climate to assess vegetation changes due to urbanization. EVI is similar to NDVI, but is more sensitive to dense vegetation than NDVI (Huete et al., 1999; Zhou et al., 2014) and less sensitive to soil and atmospheric effects (Zhang et al., 2005), thus making it extremely suitable for use in Bengaluru given its dense vegetation, high aerosol loadings, and susceptibility to monsoonal rainfall.

Bengaluru has a rapidly increasing population and increasing extent of urban areas, but its UHI intensity and corresponding impacts have not been thoroughly studied. Given Bengaluru's originally dense vegetation due to its previous nickname (i.e., "*Garden City*"), high and increasing aerosol loadings, and the fact that increasing urban temperatures can cause more heat related illnesses in a populated city, it is important to study the impacts of urbanization on surface temperature, vegetation, and aerosols together. The goals of this paper are as follows:

1. Calculate the trends of the extent of urbanized area over Bengaluru and UHI intensity during both the monsoon season and the dry season.
2. Quantify the corresponding changes in vegetation greenness and aerosol concentration for the monsoon season and the dry season over Bengaluru.
3. Understand the relationships among urbanization, UHI intensity, vegetation greenness, and aerosols for Bengaluru that could be used to project future UHI impacts.

2. Data and methods

2.1. Study region

In this study, urbanization impacts were analyzed over a 50 km × 50 km region surrounding the Bengaluru city center (12.97°N, 77.59°E). A 50 km × 50 km region was chosen such that the region would be large enough to include both urban (i.e., Bengaluru) and non-urban areas so that the UHI intensity could be calculated (i.e., urban LST minus non-urban LST). Furthermore, this study region size is small enough to exclude other urbanizing cities/towns (e.g., Town of Ramanagara that is approximately 47 km to the southwest of Bengaluru).

2.2. Precipitation seasonality

The seasonal cycle of precipitation over Bengaluru from 2003 to 2018 was analyzed to determine the months of heaviest rainfall (i.e., the monsoon season) compared to the months with the least amount of rainfall (i.e., the dry season). This time period was chosen to correspond with the availability of MODIS data (see Section 2.3). The Climate Prediction Center global unified gauge-based daily precipitation data was obtained from NOAA/OAR/ESRL/PSD from their web site https://www.esrl.noaa.gov/psd/ at 0.5° horizontal resolution. The 2003–2018 mean seasonal cycle of daily precipitation averaged over the Bengaluru region (12.25°N–13.75°N, 76.75°E–78.25°E) is shown in Fig. 1. Since the analysis is limited to a short time period, the seasonal cycle of precipitation is characterized by high internal variability. This is evidenced by the large spread between the maximum and minimum values of daily precipitation for each month. However, the monsoon season (August, September, and October–ASO) and the dry season (December, January, and February–DJF) are distinguishable since the daily mean, maximum, and minimum values were all less than 2 mm/day in DJF and there exists a rapid increase in daily precipitation right before ASO that is followed by a rapid decline. Thus, the analyses will be limited to these two seasons.
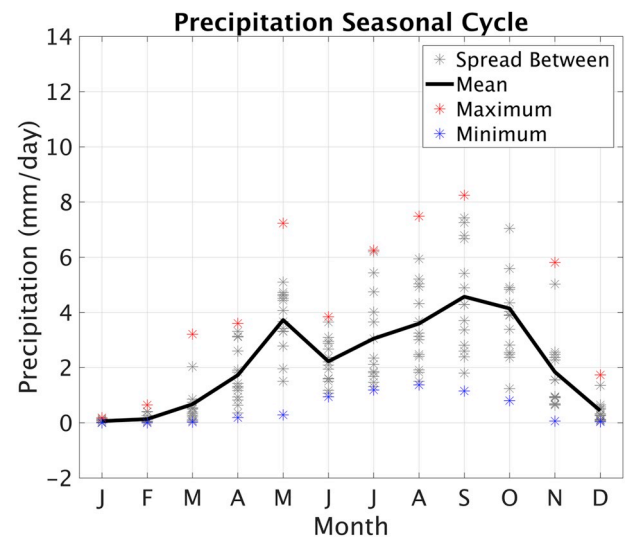

Fig. 1. The 2003–2018 mean seasonal cycle (black line) of daily precipitation averaged over Bengaluru (i.e., 12.25°N–13.75°N, 76.75°E–78.25°E), the maximum value of daily precipitation averaged over Bengaluru for each month between 2003 and 2018 (red asterisk), the minimum value of daily precipitation averaged over Bengaluru for each month between 2003 and 2018 (blue asterisk), and the spread in between the maxima and minima values (grey asterisk).

2.3. MODIS LST and land cover data

All remaining data used in this study are from MODIS instruments Terra and Aqua, which image the entire Earth's surface every 1–2 days and obtain data in 36 spectral bands that range in wavelengths from 0.4 to 14.4 μm. The sun synchronous orbital characteristics of Terra and Aqua have a daytime and nighttime Equatorial crossing time of approximately 10:30 and 13:30 local solar time, and 22:30 and 01:30, respectively. MODIS data are available since March 2000 for Terra and July 2002 for Aqua, therefore the time period of analysis was chosen to contain years 2003–2018 in order to use data from both satellites.

To quantify UHI intensity, the 8-day composite MODIS LST data at 1 km resolution from Collection 6 from both Terra (MOD11A2) and Aqua (MYD11A2) were utilized. The Terra and Aqua clear-sky measurements were combined to produce daytime LST values (averages of 10:30 and 13:30) and nighttime LST values (averages of 22:30 and 01:30). Since daily MODIS data typically suffers from orbital swath gaps and missing data, 8-day composites were used as this represents the best quality clear-sky LST measurement from all the acquisitions during each 8-day period. To identify the land cover type and quantify the land cover change over the study region, the MODIS Terra and Aqua combined annual land cover product from Collection 6 at 500 m resolution (MCD12Q1) was used. The land cover data was first re-sized to a 1 km resolution using nearest neighbor interpolation in order to match the resolution of the LST data. The 1 km MODIS land cover product (MCD12Q2) was not used since data was only available from 2003 to 2016. The MCD12Q1 500 m resolution land cover product only contained data from 2003 to 2017, therefore the land cover data from 2017 was used for 2018 since land cover type does not drastically change from year to year (i.e., Fig. 3b shows an approximate 1% yr^{-1} increase in urban land cover from 2003 to 2017).

For each year from 2003 to 2018, the 8-day MODIS LST data was utilized to calculate seasonal means for DJF and ASO. To understand where LST has changed from 2003 to 2018, linear trends in LST were computed for the entire time period for the study region in DJF and ASO during daytime and nighttime. Statistical significance of the LST trend was calculated using the Student's t-test, with a p-value ≤ 0.1 to be considered statistically significant. Although the study period of 16

years is short, the rapid urbanization has created a persistent trend and thus a linear trend is appropriate to quantify the LST changes. Note that the LST differences for the 2015–2018 mean minus the 2003–2006 mean were also calculated to illustrate the spatial patterns of LST changes. However, the results were very similar to the linear trends, and thus not shown here for brevity. Further analysis of urban heating included computing the seasonal time series of LST over the urban pixels only in an effort to characterize the change in LST attributable directly to an increase in urbanization in each year from 2003 to 2018. In order to measure the UHI intensity over time, the LST over non-urban pixels only was calculated, and then subtracted from the urban LST. It is reasonable to assume that LST over urban pixels and the LST over non-urban pixels share similar background meteorological conditions, so their LST differences reflect primarily impacts of local land surface conditions (i.e., urbanization impacts). The MODIS land cover classification for the area surrounding the Bengaluru metropolitan area is mostly croplands and does not change drastically during the time period analyzed (Fig. 2). Therefore, cropland pixels were classified as non-urban and included in the non-urban LST calculation. If a cropland pixel was within 5 km of an urban, water body, or permanent wetland pixel (i.e., transition zone from urban to non-urban), the transition region was removed from the non-urban LST calculation (e.g., Xia et al., 2019) to minimize possible contaminations (e.g., water surfaces are usually characterized by higher latent heat fluxes, and thus lower LST values).

2.4. MODIS EVI data

The 16-day composite vegetation index (VI) MODIS data for EVI at 1 km resolution from Collection 6 for 2003–2018 from both Aqua (MYD13A2) and Terra (MOD13A2) were used to measure the reduction in vegetation greenness as a result of urbanization. Data from the Aqua and Terra satellites were averaged. Similar to the LST data, the 16-day composite algorithm chooses the best available pixel value from all the clear-sky acquisitions during the 16-day period, namely the highest value acquired (Xia and Zhou, 2017). As with the LST analysis, the EVI data was utilized to calculate seasonal means for DJF and ASO for each year. EVI linear trends were assessed over the same 50 km × 50 km region surrounding the Bengaluru city center for both seasons from 2003 to 2018. Statistical significance of the EVI linear trend was calculated using the Student's t-test, with a p-value ≤ 0.1 to be considered statistically significant. The DJF and ASO mean time series of EVI over a 40 km × 40 km region surrounding the Bengaluru city center was then computed to assess the mean change in EVI over Bengaluru from 2003 to 2018. Here, the urban pixel only approach was not applied as was done for the LST analysis because it is imperative for the results to not be skewed (i.e., EVI is already low over urban pixels due to decreased vegetation abundance). A 40 km × 40 km region was chosen rather than the original 50 km × 50 km region since the most extreme surroundings are predominantly croplands and not included in the Bengaluru metropolitan area and could mask any decline in greenness over Bengaluru (e.g., Fig. 2).
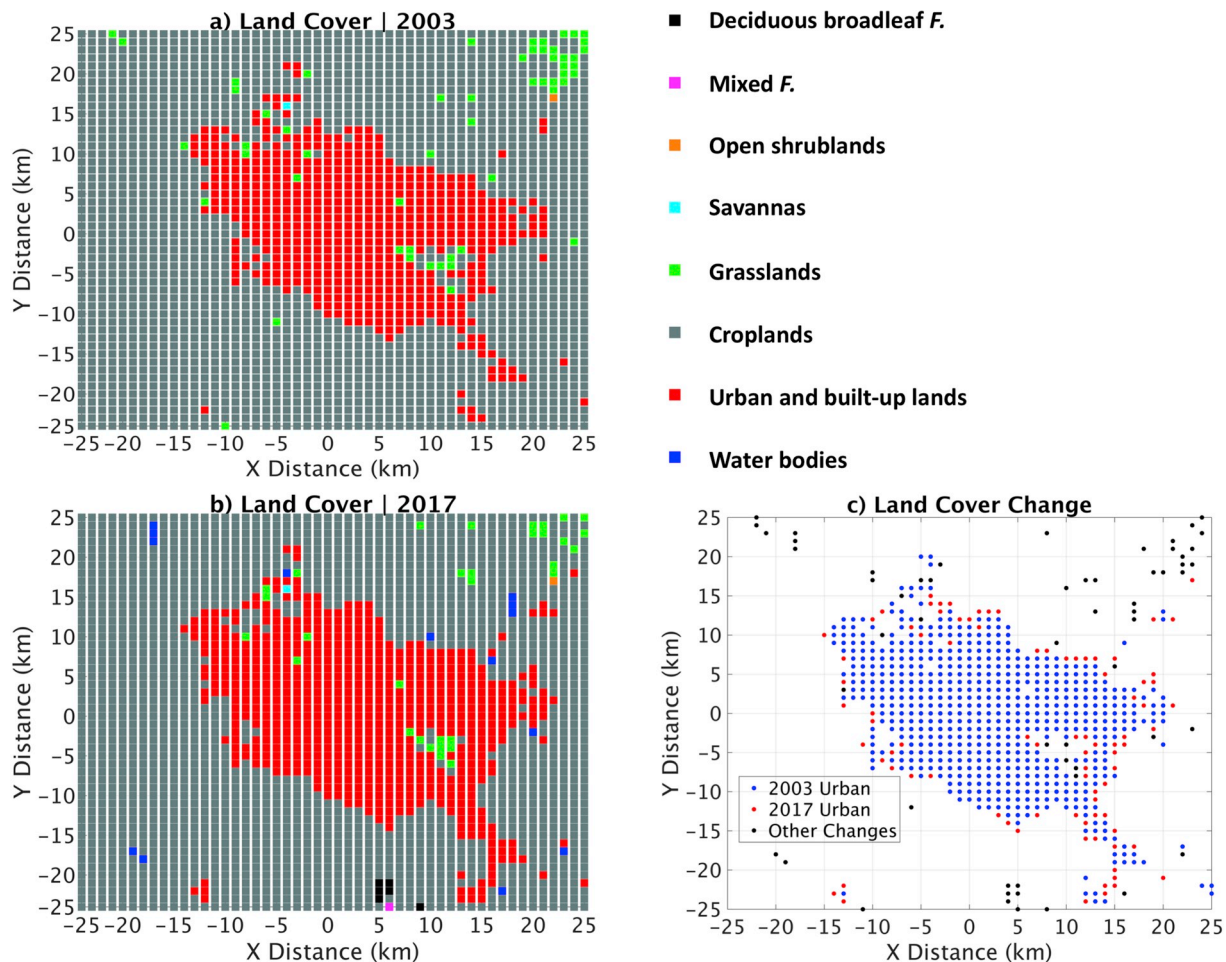

Fig. 2. The distribution of annual land cover type over the 50 km × 50 km region surrounding the Bengaluru city center for a) 2003 and b) 2017. c) The pixels associated with urban land cover in 2003 (blue stippling) and 2017 (red stippling), and other pixels that showed changes in land cover in 2017 compared to 2003 (black stippling) for the 50 km × 50 km region surrounding the Bengaluru city center. Forest has been abbreviated as *F.* in the figure legend.
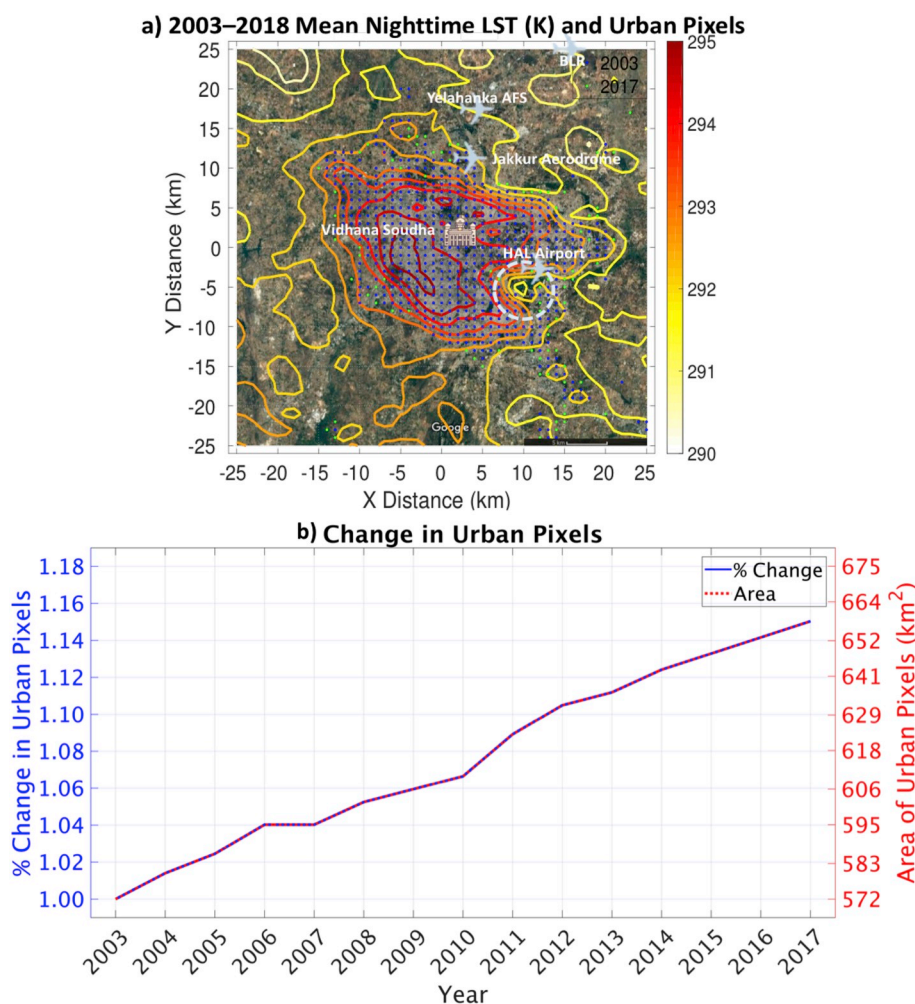
a) 2003–2018 Mean Nighttime LST (K) and Urban Pixels

b) Change in Urban Pixels

Fig. 3. a) The pixels associated with urban land cover in 2003 (blue stippling) and the additional urban pixels in 2017 (green stippling) for the 50 km × 50 km region surrounding the Bengaluru city center. Contours represent the 2003–2018 mean nighttime LST from the combined MODIS Aqua and Terra products contoured every 0.5 K from 290 K to 295 K. The landmarks pointed out include Bellandur Lake (white circle), HAL Airport, Jakkur Aerodrome, Yelahanka Air Force Station (AFS), Kempegowda International Airport Bengaluru (BLR), and Vidhana Soudha. b) The relative percentage change as compared to 2003 in the number of urban pixels over the 50 km × 50 km region over Bengaluru (blue line) and the corresponding area of urban pixels (red dashed line).

2.5. MODIS AOD data

To investigate possible impacts of increasing aerosols on UHI intensity, the MODIS Terra and Aqua combined product for AOD at a 1 km spatial resolution and daily temporal resolution (MCD19A2) was used. This product measures AOD at 0.47 μm (i.e., blue band) and 0.55 μm (i. e., green band), and measurements are made during the daytime since this remote sensing retrieval relies on solar radiation. The DJF and ASO mean time series of AOD over the 50 km × 50 km region surrounding the Bengaluru city center was computed from 2003 to 2018 to assess the trend and make any connections to UHI intensity.

3. Results

3.1. Major UHI characteristics in Bengaluru

Prior to any analysis regarding urbanization impacts, urbanization characteristics and the existence of an UHI from the chosen data were evaluated over Bengaluru. The 2003–2018 mean nighttime LST was utilized, since UHI impacts are expected to be greater at night for southern and western Asia cities (Peng et al., 2012). The urban pixel locations in 2003 and 2017 were also determined to assess where urbanization has occurred over Bengaluru (Fig. 3a). The percentage increase in urban pixels relative to 2003 for each year and the corresponding area within the 50 km × 50 km region occupied by urban pixels were also calculated (Fig. 3b). Results show that LST is higher over the Bengaluru city center when compared to the surroundings, and the coverage of urbanized area has increased by 15.03% during the time

period of interest, thereby verifying Bengaluru produces an UHI and has experienced rapid urbanization. Additionally, urbanization is mostly limited to the outskirts of Bengaluru and the urban pixel locations are co-located with the UHI (Fig. 3a). Furthermore, the LST data capture areas within the city that have lower LST. An example of this includes Bellandur Lake (white circle in Fig. 3a), which has lower LST due to higher evapotranspiration than urban surfaces.

Analysis of both the DJF and ASO 2003–2006 and 2015–2018 mean daytime LST (Fig. 4) shows a stronger UHI in ASO than in DJF for both time periods. Overall, an UHI is absent for DJF during the daytime, which may be indicative of an urban cool island since non-urban areas are characterized by higher LST than urban (Table 1). From 2003–2006 to 2015–2018, the extent of cold LST in DJF and warm LST in ASO over the urban areas has increased in magnitude and spatial extent (Fig. 4b, e). Analysis of the 2003–2018 linear trends in LST (Fig. 4c,f) illustrates a significant decrease in LST over more than two-thirds of the study region (70.12% of pixels exhibited significant changes) in DJF, and nearly all areas with a significant trend in LST in ASO are positive and situated over the pixels where urbanization has taken place on the outskirts of the city (i.e., Figs. 2c and 3a). Investigation of both the DJF and ASO 2003–2006 and 2015–2018 mean nighttime LST (Fig. 5) shows an UHI effect in both seasons that increases in magnitude and spatial extent over time. The UHI has a higher LST within the city center in ASO, however, the urban and non-urban contrast is higher in DJF (Table 1). Additionally, the UHI areal extent is greater at nighttime compared to daytime for Bengaluru. Analysis of the 2003–2018 linear trends in nighttime LST for both seasons (Fig. 5c,f) shows a significant increase in LST of approximately 1 K decade^{-1} over Bengaluru. Furthermore, the areas of
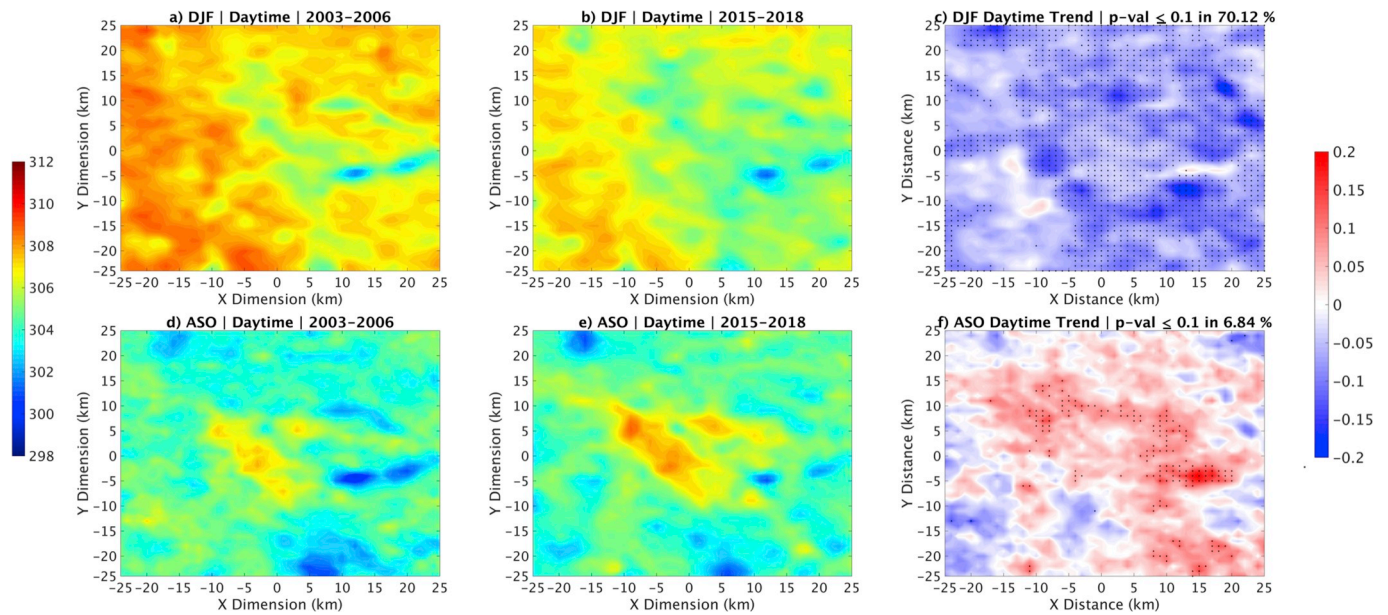
Fig. 4. a) The 2003–2006 mean daytime LST (K) for the 50 km × 50 km region surrounding the Bengaluru city center in DJF from the combined MODIS Aqua and Terra products. d) As in a), but for ASO. (b, e) As in (a, d), but for the 2015–2018 mean. c) The 2003–2018 linear trends in DJF daytime LST (K yr^{-1}). Stippling indicates where the change is statistically significant at the 10% level. f) As in c), but for ASO. The percentage of pixels that are significant are shown in the title of c) and f).

Table 1

Summary of statistics for each time series in Fig. 6. The first column represents the trend in urban, non-urban, and urban minus non-urban (i.e., UHI intensity). Bold indicates that the time series is significant as per the Mann–Kendall trend test. The second column represents the P-value of the trendline based on the Student's t-test. The last column represents the 2003–2018 mean LST value based on the time series in Fig. 6.

		LST Trend (K decade^{-1})	P-value	2003–2018 Mean (K)
DJF Daytime	Urban	**−0.94**	0.00	306.10
	Non-urban	**−0.80**	0.04	306.70
	Urban minus Non-urban	−0.14	0.34	−0.60
ASO Daytime	Urban	0.57	0.28	305.21
	Non-urban	0.15	0.82	304.07
	Urban minus Non-urban	**0.42**	0.09	1.14
DJF Nighttime	Urban	**0.39**	0.08	291.40
	Non-urban	0.18	0.50	289.97
	Urban minus Non-urban	**0.20**	0.03	1.43
ASO Nighttime	Urban	0.33	0.19	292.88
	Non-urban	0.02	0.93	291.85
	Urban minus Non-urban	**0.30**	0.02	1.02

significant LST increase again occur on the edges of the city, where the land cover changes from non-urban to urban by the end of the time period analyzed (e.g., Figs. 2c and 3a). A few non-urban areas with significant decreases in LST are also observed in both seasons (Fig. 5c,f), but further attribution over these areas is beyond the scope of this study. Note that these LST trends contain both changes in the background large-scale or regional climate change and the urban-induced signal. Since the background LST signal is large-scale and should be similar in each region and the urban areas show larger warming than non-urban except for DJF daytime, this indicates that the UHI has contributed to most of the LST warming trends.

3.2. UHI intensity

Fig. 6 shows the interannual variability and trends in UHI intensity (i.e., urban LST minus non-urban LST) from 2003 to 2018 for both DJF and ASO daytime and nighttime. Statistically significant increasing trends in UHI intensity are observed, with the exception of DJF daytime where the trend is decreasing and not significant (Fig. 6; Table 1). Here, both a Mann–Kendall (MK) trend test for each time series and a

Student's t-test for each trendline were applied to ensure the trends are robust. In each case with increasing UHI intensity, the mean urban LST has a faster increasing trend compared to the mean non-urban LST trend (Table 1) due to increased urbanization over the analyzed time period. Additionally, the 2003–2018 mean urban LST is higher than the mean non-urban LST for these cases (Table 1), thus resulting in positive mean UHI intensity. For the DJF daytime case, the mean urban LST has a faster decreasing trend compared to the mean non-urban LST trend (Table 1), thus resulting in a decreasing UHI intensity. Furthermore, the 2003–2018 mean non-urban LST is higher than the mean urban LST (Table 1), causing a negative mean UHI intensity. Note that besides urbanization, the trends in urban and non-urban LST are also affected by the regional and large-scale climate variability. However, such effects should have minor impacts on the estimate of UHI intensity because climate variability is expected to be similar across both urban and non-urban areas. For the time period of analysis, the largest urban and non-urban mean magnitude contrast occurs at nighttime during the dry season with a value of 1.43 K (Table 1). The DJF nighttime case also exhibited that fastest increasing trend in LST over urban pixels with a value of 0.39 K decade^{-1}. The UHI intensity was observed to have the
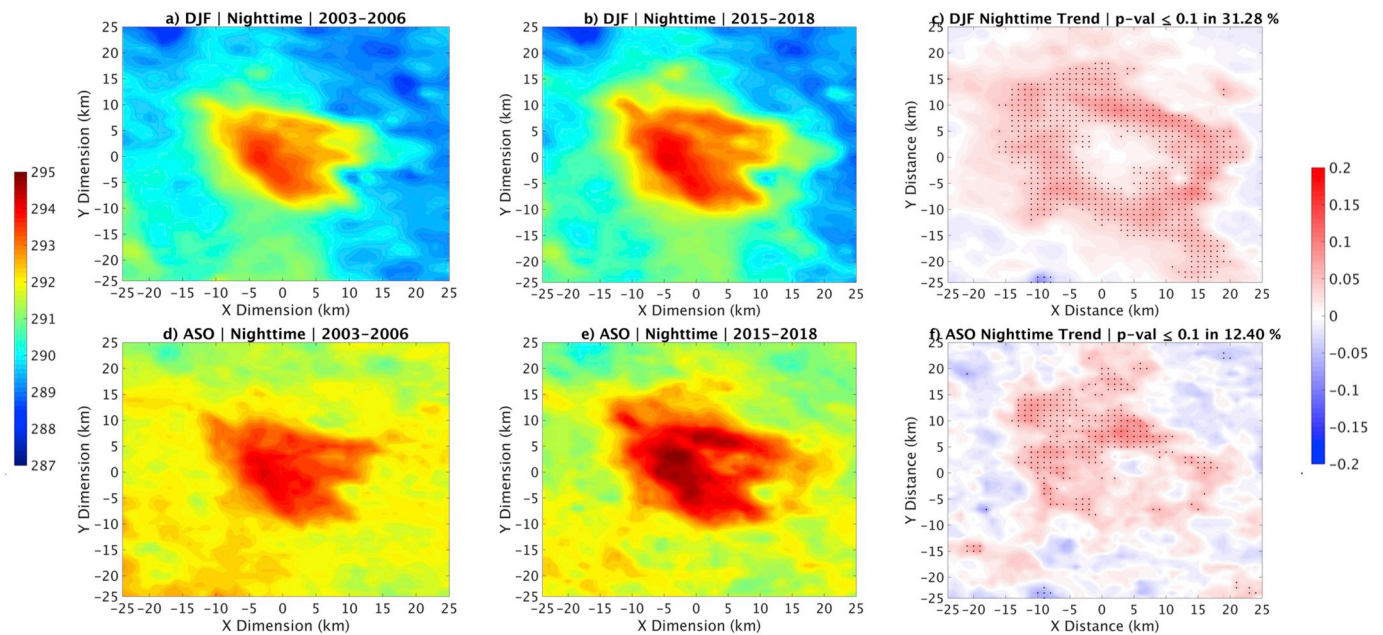
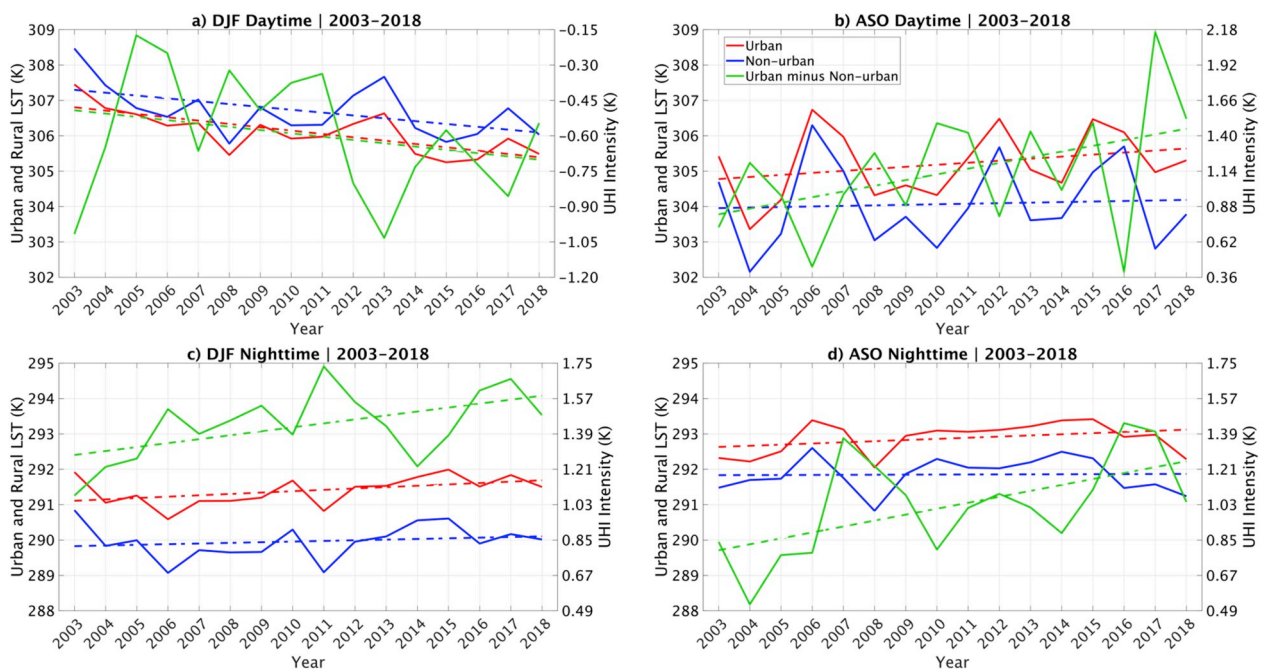**Fig. 5.** As in Fig. 4, but for nighttime LST.

Fig. 6. The time series (solid lines) and trendlines (dashed lines) of the mean urban, non-urban, and urban minus non-urban (i.e., UHI intensity) LST from the combined MODIS Aqua and Terra products for a) DJF daytime, b) ASO daytime, c) DJF nighttime, and d) ASO nighttime from 2003 to 2018. See Table 1 for trend values and significance.

fastest increasing trend in ASO daytime of 0.42 K decade^{-1}.

It is evident that the UHI in Bengaluru varies spatially and diurnally. According to Peng et al. (2012), in Asia the winter nighttime UHI intensity was higher ($1.2 \pm 0.7\,°C$) than the summer UHI nighttime intensity ($1.0 \pm 0.5\,°C$), and the summer daytime UHI intensity was higher ($1.5 \pm 1.3\,°C$) than the winter UHI daytime intensity ($0.9 \pm 1.0\,°C$). These results do coincide with the UHI intensity for Bengaluru (Table 1) in that the UHI intensity at nighttime is higher in DJF than ASO and the UHI intensity at daytime is higher in ASO than DJF. Overall, Peng et al. (2012) found the highest UHI intensity for Asia occurred in summer

daytime, while for Bengaluru the highest mean intensity occurs in winter nighttime, followed by the summer daytime. Differences in vegetation cover/amount between urban and suburban areas play a dominant role in controlling the daytime UHI intensity (Peng et al., 2012). Bengaluru was nicknamed the "*Garden City*" due to its lush greenery and presence of public parks, and thus while its vegetation is declining from urbanization, the remaining relatively high abundance of urban vegetation helps to reduce its LST contrast from its surroundings during the day. Additionally, enhanced PBL mixing over Bengaluru due to increased surface roughness also helps to weaken such LST contrast
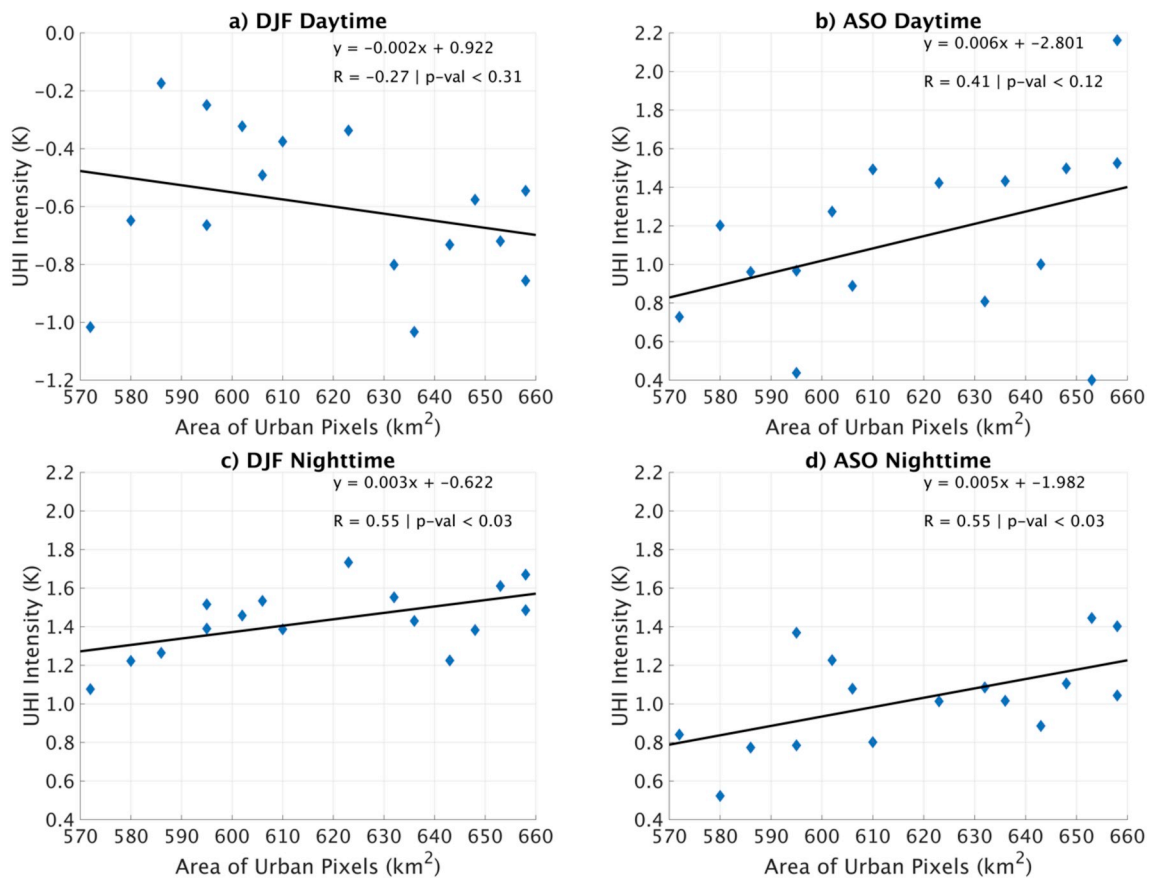
Fig. 7. Scatter plots between the area of urban pixels and the UHI intensity (i.e., urban LST minus non-urban LST) for a) DJF daytime, b) ASO daytime, c) DJF nighttime, and d) ASO nighttime. The equation of the trendline based on least squares regression and correlation coefficient (R) with p-value (*p-val*) between the area of urban pixels and the UHI intensity are shown in the top right of each panel.

during the day. These effects can possibly explain why Bengaluru's UHI does not behave in the same manner as majority of the cities assessed in Peng et al. (2012).

The empirical relationship determined between UHI intensity and the area of land that is urbanized was calculated utilizing least-squares regression (Fig. 7). Results show a positive correlation between
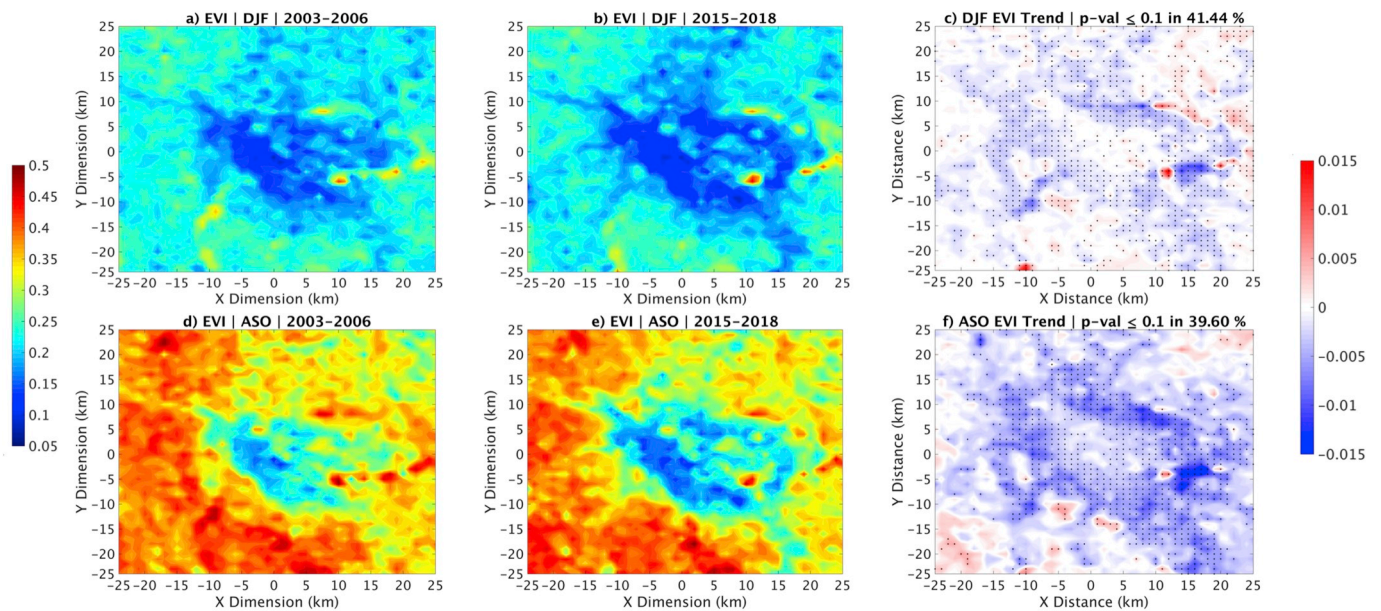

Figure 8. (a, d) The 2003–2006 mean EVI for the 50 km × 50 km region surrounding the Bengaluru city center in DJF and ASO. (b, e) As in (a, d), but for the 2015–2018 mean. (c, f) The 2003–2018 linear trends in EVI per year for DJF and ASO. Stippling indicates where the change is statistically significant at the 10% level. The percentage of pixels that are significant are shown in the title in c) and f).

increased UHI intensity and increased area of urbanized land in ASO daytime (R = 0.41), DJF nighttime (R = 0.55), and ASO nighttime (R = 0.55). However, a negative correlation occurred in DJF daytime (R = −0.27). The correlation coefficients were only significant at nighttime (p-value < 0.03 in both DJF and ASO nighttime). This linear regression model can be of great utilization for Bengaluru city planners and managers in order to determine the UHI intensity in accordance with urbanization rates. Furthermore, this model may be applicable to other tropical cities where similar urbanization growth is expected.

3.3. Impacts on vegetation greenness

EVI values are higher in ASO and have a larger range compared to DJF (Fig. 8a,b,d,e) since ASO corresponds to the wet season characterized by the peak vegetation growing season (e.g., Jiang et al., 2019). Analysis of both the average 2003–2006 and 2015–2018 EVI during both DJF and ASO (Fig. 8a,b,d,e) shows that the lowest values of EVI occur within the city center and edges. In terms of the corresponding linear trends in EVI for DJF and ASO from 2003 to 2018 (Fig. 8c,f), significant negative trends of up to −0.15 decade^{-1} within the Bengaluru city center and edges are observed. Similar to the trends in LST (Figs. 4 and 5), the negative trends are of the highest magnitude on the edges of the city, where land is becoming urbanized (i.e., Figs. 2c and 3a).

Analysis of the overall trend in the mean EVI from 2003 to 2018 for both DJF and ASO over the 40 km × 40 km region (Fig. 9) shows a significant decreasing trend in EVI of 0.01 decade^{-1} in DJF and 0.03 decade^{-1} in ASO. According to the trendlines, the relative percentage decrease in EVI in 2018 compared to 2003 is 6.32% in DJF and 13.56% in ASO. The percentage decrease in EVI during ASO is quite similar to the percentage increase in urbanization (i.e., 15.03%; Fig. 3b), which may show the strong connection between decreased vegetation and increased urbanization, and thereby increased UHI intensity. The percentage decrease in EVI during DJF is not as high as ASO due to less vegetation abundance during the dry season. Overall, these results suggest that urbanization in Bengaluru does cause a decline in vegetation greenness. Furthermore, this decline may amplify the UHI effect as more surface area transitions from vegetated to urban.

3.4. Impacts of aerosols on UHI intensity

Throughout the analysis of LST and UHI intensity, one case continuously appeared different compared to others i.e., DJF daytime. No UHI was exhibited during DJF daytime, whereas for its nighttime counterpart and for the wet season, an UHI was observed (Figs. 4 and 5). Given the notion that a high AOD can cause decreased LST by reducing the absorption of shortwave radiation at the surface (Cusack et al., 1998;
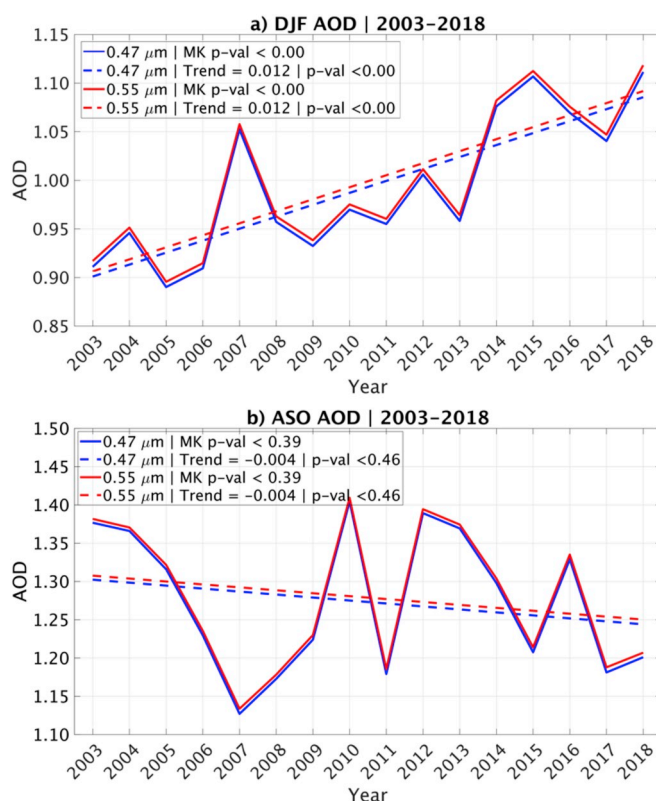

Fig. 9. The 40 km × 40 km regional average time series of EVI from 2003 to 2018 for DJF (blue) and ASO (red). The p-value from the Mann-Kendall trend test (*MK p-val*) is shown in the legend for both seasons. The slope of the trend line and p-value (*p-val*) based on the Student's t-test are also shown in the legend.

Fig. 10. a) The 50 km × 50 km regional average time series of AOD from 2003 to 2018 for DJF for 0.47 μm (blue) and 0.55 μm (red). The p-value from the Mann-Kendall trend test (*MK p-val*) as well as the slope and p-value (*p-val*) based on the Student's t-test are shown in the legend. b) As in a), but for ASO.

Lacis and Mishchenko, 1995), there exists the possibility that the decrease in LST seen during DJF daytime may be linked to an increase in AOD. On the contrary, it is likely that AOD in ASO daytime does not play a significant role in the intensity of the UHI since its intensity increases during ASO daytime.

The seasonal mean time series of AOD in DJF and ASO from 2003 to 2018 over the 50 km × 50 km region is shown in Fig. 10. Results showed a significant increase in AOD in DJF of 0.12 decade^{-1}, which is consistent with the notion that increased AOD can decrease LST. For ASO, an insignificant change in AOD occurred from 2003 to 2018 that is also characterized by high interannual variability. Aerosol trends are likely better captured and have a strong impact on LST during the winter since the boundary layer is stable, which facilitates a longer residence time of aerosol particles. On the contrary, variability in the monsoon circulation, thunderstorm activity, rainfall, and an unstable boundary layer can increase the variability of aerosol concentrations during ASO as well as cause aerosols to be removed quickly from the atmosphere by wet deposition, and thus reduce the effects of aerosols on LST during ASO (e.g., Mitchell et al., 1995). The correlation between both urban and non-urban LST and AOD in DJF was then calculated based on least-squares regression (Fig. 11) to understand their relationship. Both negative correlation coefficients are significant (p-value < 0.00 for urban LST and p-value < 0.05 for non-urban LST), thus illustrating that AOD and LST in DJF are dynamically linked. Therefore, similar to New Delhi, India, the city of Bengaluru also experiences an urban cool island during dry months due to increased AOD (Pandey et al., 2014).

4. Conclusions

This study has examined the rate of urbanization, UHI intensity, and the corresponding changes in vegetation greenness over a
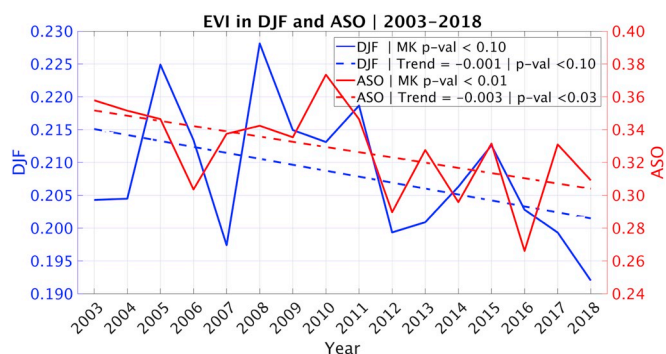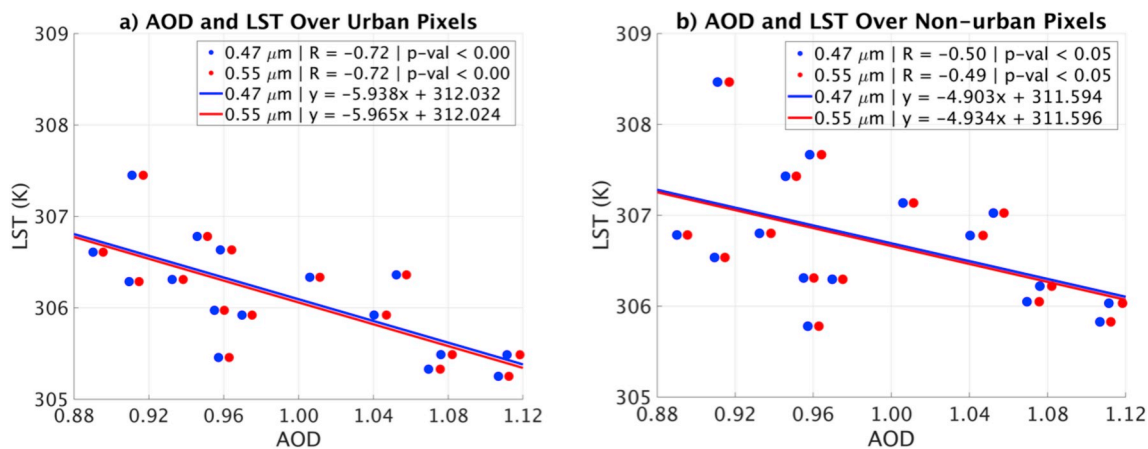
Fig. 11. a) Scatter plot between AOD measured at 0.47 μm (blue) and 0.55 μm (red) and urban LST during DJF daytime. The equation of the trendline based on least squares regression as well as the correlation coefficient (*R*) between AOD and urban LST and p-value (*p-val*) of the correlation coefficient are shown in the legend. b) As in a), but for non-urban LST.

50 km × 50 km region centered on Bengaluru, India from 2003 to 2018 in the dry and wet seasons using MODIS LST and EVI products. Results showed that the amount of urbanized land in Bengaluru increased by 15% since 2003 and the urbanization occurred on the outskirts of the city (Figs. 2 and 3). Changes in daytime and nighttime LSTs for both seasons were also quantified (Figs. 4 and 5). This analysis showed significant positive trends in LST mainly occurred near the edges of Bengaluru, i.e., where urbanization has taken place. However, a significant decreasing trend in DJF daytime LST, which is most likely linked to an increase in anthropogenic aerosols from vehicular pollution in Bengaluru (Ramachandran et al., 2012) was shown.

Further analysis of the mean seasonal UHI intensity (Fig. 6) revealed a significant increasing trend for ASO during the daytime (0.42 K decade^{-1}) and nighttime (0.30 K decade^{-1}) as well as during DJF nighttime (0.20 K decade^{-1}). While the fastest trend in UHI intensity was determined for ASO daytime, the highest 2003–2018 mean magnitude of UHI intensity was 1.43 K in DJF nighttime (Table 1). The increase in UHI intensity is also directly correlated with the area of urbanized land (Fig. 7). The corresponding changes in EVI due to urbanization were then examined (Figs. 8 and 9). A significant decrease in EVI was found, with the magnitude of the decrease being largest on the edges of Bengaluru (i.e., where urbanization took place from 2003 to 2018). The decrease in EVI was also larger in ASO (0.03 decade^{-1}) compared to DJF (0.01 decade^{-1}). The aforementioned decreasing DJF daytime LST was then further investigated using the MODIS aerosol product (Fig. 10). It was determined that an increasing AOD during DJF was linked to the decreasing daytime LST with significance for both the urban and non-urban areas (Fig. 11).

This study shows that UHI intensity has increased since 2003 in Bengaluru and is expected to continue to increase in the coming years (i. e., United Nations, 2018), with the likely exception of the daytime during DJF. Furthermore, increased urbanization has decreased vegetation greenness, and this trend will likely continue in the near-future. In addition, this study builds on the work done by Ramachandra and Kumar (2010) and Ambinakudige (2011), in that while these studies established the presence of an UHI in Bengaluru, which has caused a decrease in vegetation greenness using NDVI, a more comprehensive understanding has now been established. In this study, the diurnal cycle of the UHI for the dry and wet seasons was investigated as well as the corresponding vegetation impacts using the more suitable EVI metric. Furthermore, it was determined that Bengaluru experiences an urban cool island effect similar to New Delhi due to an increase in AOD during the dry season (Pandey et al., 2014).

This increased urbanization has the ability to impact regional and larger-scale climate. For example, Wang et al. (2012) found that

increased urbanization in China may cause an increase in incoming solar radiation due to a reduction in the cloud fraction. Also, urban areas can deepen the PBL causing water vapor to mix more evenly in the lower atmosphere, which may cause a reduction in rainfall over the urban areas due to less convective available potential energy and an increase in convective inhibition (Wang et al., 2012). An increase in air pollution due to population increase and urbanization also helps to stabilize the PBL by limiting surface warming and increasing warming at the top of the PBL. Over India, Kishtawal et al. (2010) showed areas encountering urbanization experience significantly fewer light rainfall episodes. Future work on urbanization over Bengaluru should analyze any impacts to local climate.

In the context of global warming, additional warming due to the UHI phenomenon is expected over large urban areas. In the coming years, it will be important for city planners in areas such as Bengaluru to determine ways in which to maintain vegetation greenness in order to minimize harm to vegetation and not amplify the UHI effect. Additionally, as urbanized land continues to increase in area and thus induce an UHI effect, increased temperatures may cause an increased risk for heat related illnesses and fatalities (e.g., Raghavendra et al., 2019). One way in which vegetation impacts and subsequent human health effects can be curbed is through the monitoring of green space abundance such that inhabitants can see and be a part of the natural environment as well as reduce the risks of heat exhaustion from UHI effects. For example, some local governments in China have created policies to introduce green spaces into urban environments, which has resulted in the recovery of some grasslands (Zhou and Wang, 2011). While maintaining green spaces in a time of rapid urbanization is met with difficulty (Haaland and van den Bosch, 2015), efforts are necessary since there are health benefits of green spaces, such as better mental health and lower all-cause mortality (van den Berg et al., 2015). It is recommended that cities with rapid urbanization determine the pace of their urbanization and work with environmental managers and city planners to create and/or maintain green spaces for the well-being of their inhabitants and vegetation health.

Ethical statement

All Authors declare that all ethical practices have been followed in relation to the development, writing, and publication of the article.

Author contributions

HS and AR designed the experiment and developed the methods. LZ refined the methods. HS performed the calculations and made the

figures. All authors participated in interpreting the results and drawing conclusions. HS wrote the first draft of this manuscript. AR and LZ helped revise this manuscript.

Conflict of interest

The Authors are unaware of any potential/known conflicts of interest by submitting this manuscript for publication in *Remote Sensing Applications: Society and Environment.*

Acknowledgments

References

Ambinakudige, S., 2011. Remote sensing of land cover's effect on surface temperatures: a case study of the urban heat island in Bangalore, India. Appl. GIS 7, 1–12.

Andersson, E., 2006. Urban landscapes and sustainable cities. Ecol. Soc. 11, 34.

Anniballe, R., Bonafoni, S., Pichierri, M., 2014. Spatial and temporal trends of the surface and air heat island over Milan using MODIS data. Remote Sens. Environ. 150, 163–171.

Baud, I.S.A., De Wit, J., 2008. New Forms of Urban Governance in India: Shifts, Models Networks and Contestations. Sage Publications, California.

Census of India, 2011. Karnataka District Census Handbook. Bangalore. http://censusindia.gov.in/2011census/dchb/2918_PART_A_DCHB_BANGALORE.pdf. (Accessed 2 May 2019).

Cheng, K.S., Su, Y.F., Kuo, F.T., Hung, W.C., Chiang, J.L., 2008. Assessing the effect of land cover changes on air temperature using remote sensing images – a pilot study in northern Taiwan. Landsc. Urban Plan 86, 85–96.

Cui, L., Shi, J., 2012. Urbanization and its environmental effects in Shanghai, China. Urban Clim. 2, 1–15.

Cusack, S., Slingo, A., Edwards, J.M., Wild, M., 1998. The radiative impact of a simple aerosol climatology on the Hadley Centre atmospheric GCM. Q. J. R. Meteor. Soc. 124, 2517–2526.

Dienst, M., Lindén, J., Saladié, Ò., Esper, J., 2019. Detection and elimination of UHI effects in long temperature records from villages–A case study from Tivissa, Spain. Urban Clim. 27, 372–383.

Fathi, N., Bounoua, L., Messouli, M., 2019. A satellite assessment of the urban heat island in Morocco. Can. J. Remote Sens. 45, 26–41.

Gallo, K.P., Owen, T.W., 1999. Satellite-based adjustments for the urban heat island temperature bias. J. Appl. Meteorol. Climatol. 38, 806–813.

Gallo, K.P., McNab, A.L., Karl, T.R., Brown, J.F., Hood, J.J., Tarpley, J.D., 1993. The use of NOAA AVHRR data for assessment of the urban heat island effect. J. Appl. Meteorol. Climatol. 32, 899–908.

Garratt, J.R., 1994. Review: the atmospheric boundary layer. Earth Sci. Rev. 37, 89–134.

Grimm, N.B., Faeth, S.H., Golubiewski, N.E., Redman, C.L., Wu, J., Bai, X., Briggs, J.M., 2008. Global change and the ecology of cities. Science 319, 756–760.

Haaland, C., van den Bosch, C.K., 2015. Challenges and strategies for urban green-space planning in cities undergoing densification: a review. Urban For. Urban Green. 14, 760–771.

Huete, A., Justice, C., van Leeuwen, W., 1999. MODIS Vegetation Index (MOD13) Algorithm Theoretical Basis Document, Ver. 3. http://modis.gsfc.nasa.gov/data/atbd/atbd_mod13.pdf. (Accessed 15 April 2019).

Hung, T., Uchihama, D., Ochi, S., Yasuoka, Y., 2005. Assessment with satellite data of the urban heat island effects in Asian mega cities. Int. J. Appl. Earth Obs. 8, 34–48.

Ichinose, T., Shimodozono, K., Hanaki, K., 1999. Impact of anthropogenic heat on urban climate in Tokyo. Atmos. Environ. 33, 3897–3909.

Jacobson, M.Z., 2001. Strong radiative heating due to the mixing state of black carbon on atmospheric aerosols. Nature 409, 695–697.

Jiang, Y., Zhou, L., Tucker, C.J., Raghavendra, A., Hua, W., Liu, Y., Joiner, J., 2019. Widespread increased dry season length over the Congo rainforest in the last three decades. Nat. Clim. Change 9, 617–622.

Jin, M., Shepherd, J.M., Zheng, W., 2010. Urban surface temperature reduction via the urban aerosol direct effect: a remote sensing and WRF model sensitivity study. Adv. Meteorol. 1–14.

Kalnay, E., Cai, M., 2003. Impact of urbanization and land-use change on climate. Nature 423, 528–531.

Kanakidou, M., Mihalopoulos, N., Kindap, T., Im, U., Vrekoussis, M., Gerasopoulos, E., Dermitzaki, E., Unal, A., Koçak, M., Markakis, K., Melas, D., Kouvarakis, G., Youssef, A.F., Richter, A., Hatzianastassiou, N., Hilboll, A., Ebojie, F., Wittrock, F., von Savigny, C., Burrows, J.P., Ladstaetter-Weissenmayer, A., Moubasher, H., 2011. Megacities as hot spots of air pollution in the East Mediterranean. Atmos. Environ. 45, 1223–1235.

Kim, Y.H., Baik, J.J., 2002. Maximum urban heat island intensity in Seoul. J. Appl. Meteorol. Climatol. 41, 651–659.

Kim, Y.H., Baik, J.J., 2005. Spatial and temporal structure of the urban heat island in Seoul. J. Appl. Meteorol. Climatol. 44, 591–605.

Kishtawal, C.M., Niyogi, D., Tewari, M., Pielke, R.A., Shepherd, J.M., 2010. Urbanization signature in the observed heavy rainfall climatology over India. Int. J. Climatol. 30, 1908–1916.

Koelmans, A.A., Jonker, M.T.O., Cornelissen, G., Bucheli, T.D., van Noort, P.C.M., Gustafsson, Ö., 2006. Black carbon: the reverse of its dark side. Chemosphere 63, 365–377.

Lacis, A.A., Mishchenko, M.I., 1995. Climate forcing, sensitivity, and response. In: Charlson, R.J., Heintzenberg, J. (Eds.), Aerosol Forcing of Climate. John Wiley, Chichester, UK, pp. 11–42.

Latha, K.M., Badarinath, K.V.S., 2003. Black carbon aerosols over tropical urban environment–a case study. Atmos. Res. 69, 125–133.

Latha, K.M., Badarinath, K.V.S., 2005. Seasonal variations of black carbon aerosols and total aerosol mass concentrations over urban environment in India. Atmos. Environ. 39, 4129–4141.

Mendelsohn, R., Kurukulasuriya, P., Basist, A., Kogan, F., Williams, C., 2007. Climate analysis with satellite versus weather station data. Clim. Change 81, 71–83.

Miao, S., Chen, F., LeMone, M., Tewari, M., Li, Q., Wang, Y., 2009. An observational and modeling study of characteristics of urban heat island and boundary layer structures in Beijing. J. Appl. Meteorol. Climatol. 48, 484–501.

Mitchell, J.F.B., Davis, R.A., Ingram, W.J., Senior, C.A., 1995. On surface temperature, greenhouse gasses, and aerosols: models and observations. J. Clim. 8, 2364–2386.

Mostovoy, G.V., King, R.I., Reddy, K.R., Kakani, V.G., Filippova, M.G., 2006. Statistical estimation of daily maximum and minimum air temperatures from MODIS LST data over the state of Mississippi. GISci. Remote Sens. 43, 78–110.

Oke, T.R., 1973. City size and the urban heat island. Atmos. Environ. 7, 769–779.

Pandey, A.K., Singh, S., Berwal, S., Kumar, D., Pandey, P., Prakash, A., Lodhi, N., Maithani, S., Jain, V.K., Kumar, K., 2014. Spatio–temporal variations of urban heat island over Delhi. Urban Clim. 10, 119–133.

Park, H.-S., 1986. Features of the heat island in Seoul and its surrounding cities. Atmos. Environ. 20, 1859–1866.

Peng, S., Piao, S., Ciais, P., Friedlingstein, P., Ottle, C., Bréon, F.M., Nan, H., Zhou, L., Myneni, R.B., 2012. Surface urban heat island across 419 global big cities. Environ. Sci. Technol. 46, 696–703.

Petersen, T.C., 2003. Assessment of urban versus rural in situ surface temperatures in the Contiguous United States: No difference found. J. Clim. 16, 2941–2959.

Prihodko, L., Goward, S.N., 1997. Estimation of air temperature from remotely sensed surface observations. Remote Sens. Environ. 60, 335–346.

Qian, Y., Leung, R., Ghan, S.J., Giorgi, F., 2003. Regional climate effects of aerosols over China:Modeling and observations. Tellus B 55, 914–934.

Qian, Y., Kaiser, D.P., leung, L.R., Xu, M., 2006. More frequency cloud-free sky and less surface solar radiation in China from 1955 to 2000. Geophys. Res. Lett. 33, L01812.

Raghavendra, A., Dai, A., Milrad, S.M., Cloutier-Bisbee, S.R., 2019. Floridian heatwaves and extreme precipitation: future climate projections. Clim. Dyn. 52, 495–508.

Ramachandra, T.V., Kumar, U., 2010. Greater Bangalore: emerging urban heat island. GIS Develop. 4, 86–104.

Ramachandran, S., Kedia, S., 2010. Black carbon aerosols over an urban region: radiative forcing and climate impact. J. Geophys. Res. 115, D10202.

Ramachandran, S., Kedia, S., Srivastava, R., 2012. Aerosol optical depth trends over different regions of India. Atmos. Environ. 49, 338–347.

Safai, P.D., Kewat, S., Praveen, P.S., Rao, P.S.P., Momin, G.A., Ali, K., Devara, P.C.S., 2007. Seasonal variation of black carbon aerosols over a tropical urban city of Pune, India. Atmos. Environ. 41, 2699–2709.

Schwarz, N., Schlink, U., Franck, U., Großmann, K., 2012. Relationship of land surface and air temperatures and its implications for quantifying urban heat island indicators – an application for the city of Leipzig (Germany). Ecol. Indic. 18, 693–704.

Streutker, D.R., 2003. Satellite-measured growth of the urban heat island of Houston, Texas. Remote Sens. Environ. 85, 282–289.

Sudhira, H.S., Nagendra, H., 2013. Local assessment of Bangalore: graying and greening in Bangalore–Impacts of urbanization on ecosystems, ecosystem services and biodiversity. In: Elmqvist, T. (Ed.), Urbanization, Biodiversity and Ecosystem Services: Challenges and Opportunities: A Global Assessment. Springer, Netherlands, pp. 75–91.

Sudhira, H.S., Ramachandra, T.V., Bala Subrahmanya, M.H., 2007. City profile: Bangalore. Cities 24, 379–390.

Taha, H., 1997. Urban climates and heat islands: albedo, evapotranspiration, and anthropogenic heat. Energy Build. 25, 99–103.

Tie, W., Cao, J., 2009. Aerosol pollution in China: present and future impact on environment. Particuology 7, 426–431.

United Nations, 2018. World urbanization prospects – 2018 revision. https://population.un.org/wup/. (Accessed 29 April 2019).

van den Berg, M., Wendel-Vos, W., van Poppel, M., Kemper, H., van Mechelen, W., Maas, J., 2015. Health benefits of green spaces in the living environment: a systematic review of epidemiological studies. Urban For. Urban Green. 14, 806–816.

Wang, J., Feng, J., Yan, Z., Hu, Y., Jia, G., 2012. Nested high-resolution modeling of the impact of urbanization on regional climate in three vast urban agglomerations in China. J. Geophys. Res. 117, D21103.

Weng, Q.H., Lu, D.S., Schubring, J., 2004. Estimation of land surface temperature-vegetation abundance relationship for urban heat island studies. Remote Sens. Environ. 89, 467–483.

Xia, G., Zhou, L., 2017. Detecting wind farm impacts on local vegetation growth in Texas and Illinois using MODIS vegetation greenness measurements. Remote Sens. 9, 698.

Xia, G., Zhou, L., Freedman, J.M., Roy, S.B., Harris, R.A., Cervarich, M.C., 2016. A case study of effects of atmospheric boundary layer turbulence, wind speed, and stability on wind farm induced temperature changes using observations from a field campaign. Clim. Dyn. 46, 2179–2196.

Xia, G., Zhou, L., Minder, J.R., Fovell, R.G., Jiménez, P.A., 2019. Simulating impacts of real-world wind farms on land surface temperature using WRF model: physical Mechanisms. Clim. Dyn. 53, 1723–1739.

Yang, P., Ren, G., Liu, W., 2013. Spatial and temporal characteristics of Beijing urban heat island intensity. J. Appl. Meteorol. Climatol. 52, 1803–1816.

Zhang, X., Friedl, M.A., Schaaf, C.B., Strahler, A.H., Liu, Z., 2005. Monitoring the response of vegetation phenology to precipitation in Africa by coupling MODIS and TRMM instruments. J. Geophys. Res. 110, D12103.

Zhou, X., Wang, Y.C., 2011. Spatial–temporal dynamics of urban green space in response to rapid urbanization and greening policies. Landsc. Urban Plan. 100, 268–277.

Zhou, L., Dickinson, R.E., Tian, Y.H., Fang, J.Y., Li, Q.X., Kaufmann, R.K., 2004. Evidence for a significant urbanization effect on climate in China. Proc. Natl. Acad. Sci. 101, 9540–9544.

Zhou, L., Dickinson, R.E., Tian, Y., Vose, R.S., 2007. Impact of vegetation removal and soil aridation on diurnal temperature range in a semiarid region – application to the Sahel. Proc. Natl. Acad. Sci. U.S.A. 104, 17937–17942.

Zhou, L., Tian, Y., Myneni, R.B., Ciais, P., Saatchi, S., Liu, Y.Y., Piao, S., Chen, H., Vermote, E.F., Song, C., Hwag, T., 2014. Widespread decline of Congo rainforest greenness in the past decade. Nature 509, 86–90.

Zhou, L., Tucker, C.J., Kaufmann, R.K., Slayback, D., Shabanov, N.V., Myneni, R.B., 2001. Variations in northern vegetation activity inferred from satellite data of vegetation index during 1981 to 1999. J. Geophys. Res. 106, 20069–20083.